Position Control of Mobile Robot for Human-Following in Intelligent Space with Distributed Sensors

Tae-Seok Jin, Jang-Myung Lee, and Hideki Hashimoto

Abstract: Latest advances in hardware technology and state of the art of mobile robot and artificial intelligence research can be employed to develop autonomous and distributed monitoring systems. And mobile service robot requires the perception of its present position to coexist with humans and support humans effectively in populated environments. To realize these abilities, robot needs to keep track of relevant changes in the environment. This paper proposes a localization of mobile robot using the images by distributed intelligent networked devices (DINDs) in intelligent space (ISpace) is used in order to achieve these goals. This scheme combines data from the observed position using dead-reckoning sensors and the estimated position using images of moving object, such as those of a walking human, used to determine the moving location of a mobile robot. The moving object is assumed to be a point-object and projected onto an image plane to form a geometrical constraint equation that provides position data of the object based on the kinematics of the intelligent space. Using the a priori known path of a moving object and a perspective camera model, the geometric constraint equations that represent the relation between image frame coordinates of a moving object and the estimated position of the robot are derived. The proposed method utilizes the error between the observed and estimated image coordinates to localize the mobile robot, and the Kalman filtering scheme is used to estimate the location of moving robot. The proposed approach is applied for a mobile robot in ISpace to show the reduction of uncertainty in the determining of the location of the mobile robot. Its performance is verified by computer simulation and experiment.

Keywords: Intelligent space, localization, mobile robot, moving object, uncertainty.

1. INTRODUCTION

This document is a during the past two decades, researchers from the field of mobile robotics have dealt with different path planning methods. In most cases, the goal of the methods is to determine collision-free paths that will meet the initial and final configurations to accomplish a mission. Some researchers have proposed methods in where the precise configuration of the robot is known at each instant during the planning and navigation stages [1]. However, this is not always possible. It is essential to deal with uncertainty in the planning stage when the values of position errors approach the allowed thresholds for the mission. Plans based on geometrical models, assuming null uncertainty, are clearly insufficient when the mobile robot has to coexist with humans or in other types of difficult situations. Thus, the use of planners, which does not explicitly deal with uncertainty, is limited to simple situations where the errors are less than the allowed thresholds to accomplish the mission [2]. Generally, the basic requirements for the autonomous navigation of a mobile robot are environmental recognition, path planning, driving control, and location estimation/ correction capabilities [6,7]. The location estimation and correction capabilities are practically indispensable for the autonomous mobile robot to execute the given tasks efficiently. There are several factors involved in obtaining accurate location information while the mobile robot is moving [16]. To obtain reliable and precise location data, sensor fusion techniques [8,20] have also been developed. When a CCD camera is utilized under good illumination

Manuscript received December 18, 2004; revised September 23, 2005 and November 22, 2005; accepted December 12, 2005. Recommended by Editorial Board member Fumitoshi Matsuno under the direction of Editor Keum-Shik Hong.

Tae-Seok Jin is with the Dept. of Mechatronics Engineering, DongSeo University, San 69-1 Churye-dong, Sasang-ku, Busan 617-716, Korea (e-mail: jints@dongseo.ac.kr).

Jang-Myung Lee is with the School of Electronics Engineering, Pusan National University, San 30 Jangjeon-dong, Geumjeong-ku, Busan 609-735, Korea (e-mail: jmlee@ pusan.ac.kr).

Hideki Hashimoto is with the Institute of Industrial Science, the University of Tokyo, 4-6-1 Komaba, Meguro-ku, Tokyo 153-8505, Japan (e-mail: hashimoto@iis.u-tokyo.ac.jp).

conditions, certain patterns or shapes of objects also enable effective determination of the location [11,23]. Similarly, when a mobile robot is moving in a building, the walls, edges, and doors can be utilized for position estimation [3,4]. Most researches [22-24] focus on the indoor navigation of a mobile robot in a well-structured environment. In other words, beacons, doors, and corridor edges are utilized to estimate the current location of the mobile robot. However, in cases wherein a mobile robot is navigating under a deep sea or in a forest [17], there are no landmarks that can be utilized to determine the location.

This paper considers the situations in which a mobile robot and a walking human coexist in a structured intelligent environment, such as an assembly line in a factory. In these cases, one cannot utilize any landmarks or special features known a priori [14,19] to localize the mobile robot. The only data that can be utilized for the localization is information on the human captured by a CCD camera attached to the top of the mobile robot. An intelligent environment is used to solve these problems, and a new scheme for the mobile robot localization using information about the moving object has been developed. This situation may be considered to be the opposite of tracking an unknown moving object using a camera- equipped navigating robot. The location of the robot is precisely calibrated and stored at the times. The tracking problem has been already tackled in many researches studies [13,21].

In this research, the data obtained from the dead reckoning sensors are used to determine the initial location of the mobile robot, and it is corrected through the position estimation procedure using the information on the moving object/walking human. In the quantitative analysis of this approach, the position uncertainty of the mobile robot [15,18] is represented by an uncertainty ellipsoid that quantitatively shows the directional uncertainty. To reduce the size of the uncertainty ellipsoid, the trajectory of the moving object is transformed to the image frame and represented as a geometrical constraint equation, which is used for the Kalman filtering process [9,10] that estimates the position of the mobile robot. A mobile robot interacts with multiple intelligent sensors, which are distributed in the environment. The distributed sensors recognize the mobile robot and the moving object/walking human, and they issue control commands to the mobile robot. The mobile robot receives the necessary support for localization control from the environmental sensors. We aim to perform the localization of a mobile robot which is simple in structure, without laying any burden on the human who is in its vicinity. We propose intelligent space (ISpace) as an environment with several intelligent sensors, and we are building an environment wherein humans and mobile robots can coexist. In this research, the mobile robot is one of the physical agents for human support in the ISpace [25,26].

This paper is organized as follows. In Section 2, the concepts of ISpace and robot localization in intelligent space are explained. Section 3 describes the driving model of a mobile robot and the position estimation uncertainty. In Section 4, the image transformation relation, the image projection of the human-walking trajectory, and the position correction technique using the Kalman filter are described. Section 5 explains the proposed control method as applied to the ISpace. Simulations and experiments of robot localization are performed and the effect of the proposed method is verified. Finally, the conclusions and directions for future work are described in Section 6.

2. ROBOT LOCALIZATION IN ISPACE

2.1. Structure of ISpace

As shown in Fig. 1, ISpace [25] is a space throughout which several intelligent devices are distributed. These intelligent devices have sensing, processing, and networking functions, and they are termed distributed intelligent networked devices (DINDs). These devices observe the positions and behavior of both humans and robots that coexist in the ISpace. The information acquired by each DIND is shared with the other DINDs through the network communication system. Based on the accumulated information, the environment as a system is capable of understanding the actions of humans. In order to support humans, the environment/system utilizes machines including computers and robots.

2.2. Multi-camera ISpace system

In the ISpace, the CCD camera is adopted as the sensor for the DINDs, and moving objects, such as walking humans, and mobile robots, are tracked. The use of CCD cameras offers two advantages: the

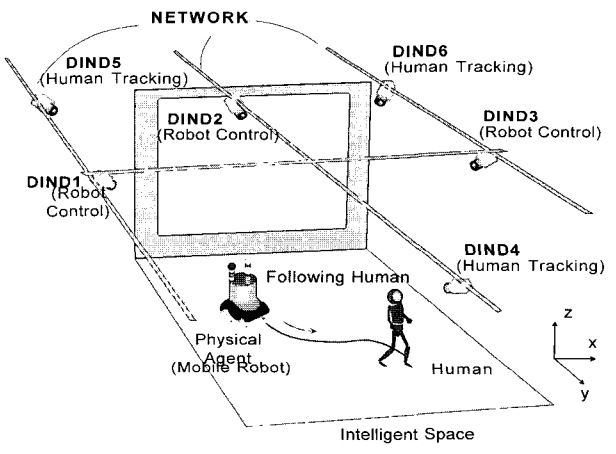

Fig. 1. Structure of the intelligent environment obtained by distributed cameras.

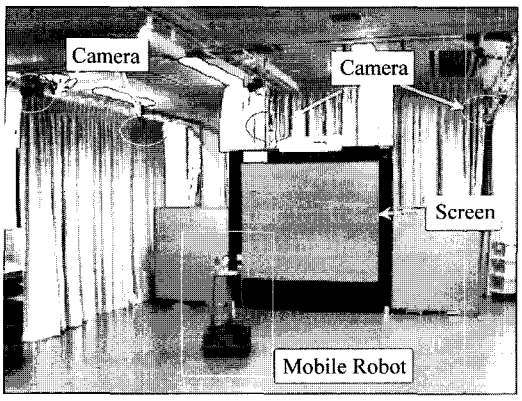

Fig. 2. Experimental environment - ISpace.

position measurement of the targets is obtained using a non-contact method, and the human need not be equipped with any special devices for the DINDs to be able to measure his position. A laboratory, approximately 7m in both width and depth, is used as the ISpace and experiments were performed in it. The ISpace has a mobile robot as a human-following agent, six DINDs that can obtain information on the environment, and a projector and screen that provide the human with necessary information. Each module is connected through the network communication system. Three DINDs are used to recognize the mobile robot and generate the control commands. The other three DINDs are used to recognize the position of the human. The DINDs are placed as shown in Fig. 1.

Fig. 2 is an image of the actual ISpace. The placement of the three DINDs for human recognition is optimized in order to expand the viewable area of the cameras and recognize the head and hands of the human over a wide area [12]. On the other hand, the placement of the DINDs for the mobile robot recognition has to be determined by trial and error. In order to achieve a human-following system and reliable mobile robot control, it is desirable that the DINDs for the mobile robot recognize the entire area covered by the three DINDs associated with human recognition. Thus, the three DINDs for the mobile robot are placed such that the area for human recognition is completely covered. Information on the walking human is extracted by background subtraction and by detecting the skin color of the face and hands on captured images.

As shown in Fig. 3, a mobile robot is connected to the DIND network via wireless LAN, and it shares the resources of the DINDs. In order to recognize the position of the robot, one-color panels are installed around the mobile robot. The pattern of the color panel is recognized by a DIND, and the posture and position of the robot are estimated by the kinematics of the robot projected onto an image plane. Since the height of the mobile robot is already known, the position of the mobile robot is reconstructed from a single camera image.

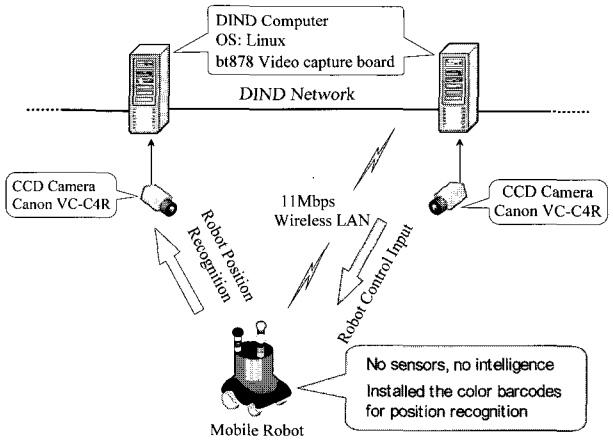

Fig. 3. Mobile robot and network system in the ISpace.

2.3. Robot control by DINDs

The human-following module of a DIND is realized by software configuration [25]. The network of six DINDs, which consist of three DINDs for the mobile robot and three DINDs for the human, is used in the experimental environment. Since each DIND is capable of covering limited area, the DINDs must share the information they acquire in order to realize human following across the entire experimental environment.

In this environment, the DINDs are required to cooperate with each other. Effective communication and role assignment are essential for the cooperation of the DINDs. The dominant DIND for the robot is defined as the one that possesses control authority over a robot. Each DIND compares its reliability rank based on the measurement error and other factors. When a robot moves from one area to another, the dominant DIND for the robot needs to be switched automatically to the DIND that has a higher reliability rank. This is termed handing over [26] the control authority. The dominant DIND possesses the control authority of the robot, and only one dominant DIND exists for a given robot at any given time instant. The

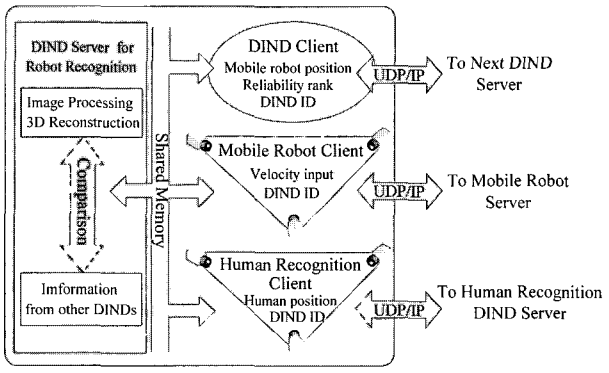

Fig. 4. Network configuration of the DIND.

human-following module of a DIND is realized with the software configuration shown in Fig. 4.

2.4. Basic concept of robot localization in ISpace

The basic concepts for the robot localization in ISpace are described in this subsection. A new scheme is proposed for a mobile robot to estimate and change its position for following human using the human images obtained by the cameras in ISpace. The position of a walking human and a mobile robot were estimated using the kinematics of the camera adopted as the sensor in ISpace and the images of the mobile robot assuming that it is point object and the size of point is set to 30cm x 100cm, respectively.

In order to plan the uncertainty reduction for the robot to estimate and follow the walking human, the linear and angular velocities of the walking human were estimated for the human-following robot to relocate using the trajectory of the human. A state estimator was designed using a Kalman filter to overcome the uncertainties in the image data caused by the point-object assumption and physical noises. Based on the motion information of the walking human, the human-following robot was controlled to improve its own position estimation accuracy by observing the walking human.

3. POSITION UNCERTAINTY MODELING

3.1. First part

The initial position of a mobile robot can be specified precisely. However, measurement error and slippage during movement may lead to a large position estimation uncertainty. This uncertainty increases with driving distance, and eventually, the location of the mobile robot may be lost.

The robot's position is represented by the vector of its spatial variables $\mathbf{x}(k)$ as a point in the Cartesian plane, with $x_r(k)$ and $y_r(k)$ as the coordinates and an orientation of $\theta_r(k)$, $\mathbf{x} = [x_r, y_r, \theta_r]^T$. The simplified kinematic model proposed in [15] describes how the robot's position changes with time in relation to an initial position and in response to a control input $\mathbf{u}(k)$ formed by a translation $T(k)$ followed by a rotation $\theta_r(k)$: $\mathbf{u}(k) = [T(k), \theta_r(k)]^T$. The state for a given instant is obtained from the state transition function $f(\mathbf{x}(k), \mathbf{u}(k))$, represented in (1) as follows:

$$\begin{aligned}\mathbf{x}(k+1) &= f(\mathbf{x}(k), \mathbf{u}(k)) + \mathbf{v}(k) \\ &= \begin{bmatrix} x_r(k) + T(k)\cos(\theta_r(k)) \\ y_r(k) + T(k)\sin(\theta_r(k)) \\ \theta_r(k) + \Delta\theta(k) \end{bmatrix} + \mathbf{v}(k),\end{aligned} \tag{1}$$

where $f(\mathbf{x}(k), \mathbf{u}(k))$ is a non-linear state transition function, $\mathbf{v}(k)$ is a noise source assumed to be zero-mean Gaussian with covariance $\mathbf{Q}(k) \rightarrow N(0, Q(k))$, and $\mathbf{u}(k)$ is the control input. The position uncertainty of the robot is modeled by means of a Gaussian distribution of probability centered in the vehicle position at a given moment. (1) to obtain the mean vector estimation in the $k + 1$ position. Next, tt is necessary to estimate the covariance matrix in the same position. The first two moments that follow the spatial position relationship, namely the mean and the covariance of the distribution function, must be determined. The covariance matrix related to the prediction in the case of non-linear spatial relationship is obtained from the Taylor series expansion. Therefore, the estimated position of a mobile robot and $\hat{\mathbf{x}}(k \mid k)$ covariance matrix equation are represented in (2) and (3), respectively [9], as

$$\hat{\mathbf{x}}(k+1) = f(\hat{\mathbf{x}}(k), \mathbf{u}(k)), \tag{2}$$

$$\mathbf{P}(k+1 \mid k) = \nabla\mathbf{f}\, \mathbf{P}(k \mid k) \nabla\mathbf{f}^T + \mathbf{Q}(k), \tag{3}$$

where $\nabla\mathbf{f}$ is the Jacobian of the state transition function, obtained as the linearizing result around the estimated state. The Jacobian of the state transition function is described in (4) as follows:

$$\nabla\mathrm{f} = \begin{bmatrix} 1 & 0 & T(k)\sin(\hat{\theta}_r(k \mid k)) \\ 0 & 1 & T(k)\cos(\hat{\theta}_r(k \mid k)) \\ 0 & 0 & 1 \end{bmatrix}. \tag{4}$$

In order to estimate the vehicle position, odometry is insufficient. The $\hat{x}(k \mid k)$ covariance matrix equation represented in (3) tends to grow continuously (Fig. 6). Using this covariance matrix, the position estimation uncertainty can be represented as a hyper-ellipsoid. In other words, the uncertainty hyper-ellipsoid can be defined [6] based on the singular value decomposition (SVD) of the covariance matrix. This SVD provides the principal axis by the left singular vectors and the length along the axis by the

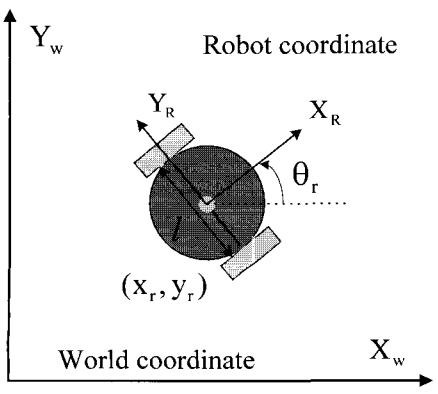

Fig. 5. Geometrical model of a mobile robot.

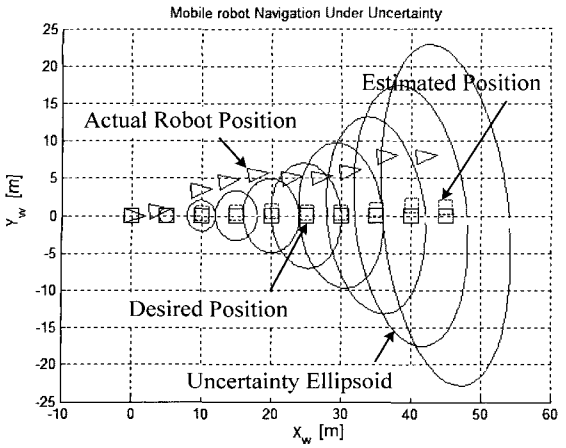

Fig. 6. Uncertainty ellipsoids with the movement of a mobile robot. above form.

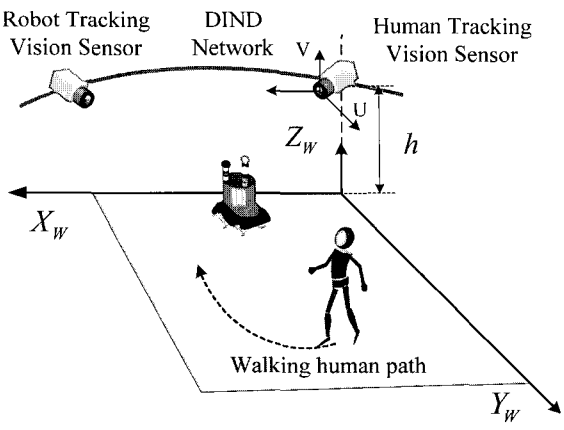

Fig. 7. Coordinates for a walking object and a mobile robot.

corresponding singular values. As an example, Fig. 6 illustrates the effectiveness of the uncertainty ellipsoid. It indicates that the uncertainty ellipsoid becomes larger with the movement of a mobile robot and the geometrical shape of the ellipsoid directly represents the position estimation uncertainty along a given axis.

4. POSITION ESTIMATION BASED ON DINDS

4.1. Image projection of a walking human

During navigation, a mobile robot may need to relocate. When the image of a walking human is captured by the CCD cameras of DINDs and the motion information on the walking human is available to the mobile robot, it may halt at its current position to improve its own position estimation accuracy by observing the walking human. Using the current position estimation of the mobile robot, the given object trajectory can be represented as a linear equation in the image frame and geometric constraint equations can be derived through coordinate transformation.

The derivation procedure of the geometric constraint equations is illustrated with an example in Fig. 7. The conventional pin-hole model [7] is utilized to form a geometrical model of the camera. In Fig. 7, (x_W y_W z_W) and (u, v) represent the reference coordinates and the image coordinates, respectively. The trajectory of the walking human on the $x_W - y_W$ plane of the reference coordinates, without loss of generality, is assumed to be as follows

$$f(x_W, y_W) = 0, \tag{5}$$

$z_W (= z_0 \neq h)$ is also assumed to be constant and not equal to the camera height, h.

The walking human trajectory in the reference coordinates can then be transformed into the robot coordinates, as follows:

$$\begin{bmatrix} x_R \\ y_R \\ z_R \end{bmatrix} = \begin{bmatrix} \cos\hat{\theta}_r & \sin\hat{\theta}_r & 0 \\ -\sin\hat{\theta}_r & \cos\hat{\theta}_r & 0 \\ 0 & 0 & 1 \end{bmatrix} \begin{bmatrix} x_W - \hat{x}_r \\ y_W - \hat{y}_r \\ z_W \end{bmatrix}, \tag{6}$$

where $[\hat{x}_r\ \hat{y}_r\ \hat{z}_r]^T$ represents the current estimated position of the mobile robot and $[x_W\ y_W\ z_W]^T$ represents the position of the walking human. This point ($[x_R\ y_R\ z_R]^T$) is mapped once more onto the image frame using perspective projection, as follows [7,11]:

$$\begin{bmatrix} u \\ v \end{bmatrix} = \begin{bmatrix} \lambda \dfrac{y_R}{x_R} \\ \lambda \dfrac{z_R - h}{x_R} \end{bmatrix}, \tag{7}$$

where λ represents the camera focal length and $z = [u\ \ v]^T$ is the position of the walking human on the image frame. Based on (6) and (7), the geometric constraint equation can be generally represented as

$$f(z, \hat{x}) = 0, \tag{8}$$

where $\hat{x} = [\hat{x}_r, \hat{y}_r, \hat{z}_r]^T$ represents the current estimated position of the mobile robot.

4.2. Position correction

There is some discrepancy between the calculated position of the walking human in the image frame, which is based on the estimated robot position, and the actual value. Utilizing this error, the real position of the robot can be corrected recursively. To overcome vague input information, i.e., the noise of

the human position in the image frame and uncertainty components of the position estimation of the robot, the Kalman filtering technique is adopted to develop a robust observer [9,10]. The geometric constraint equations between the human image coordinates and the robot position are approximated to a linear equation, and the Kalman filtering technique is applied to estimate the position of moving robot. It is assumed that the i[th] measured vector, i.e., the position of the walking human, $\hat{z}_i$, includes noise with the following average and variance:

$$\hat{z}_i = z_i + v_i, \tag{9}$$

where $E[\ v_i] = 0$ and $E[v_i v_i^T] = S_i$.

Using the Taylor series expansion and ignoring the higher order nonlinear terms at the measured vector, $\hat{z}_i$, and the estimated position of the mobile robot, $\hat{x}_{i-1}$, the nonlinear constraint equations are approximated to linear equation as follow:

$$\begin{aligned} & f(z_i, \hat{x}) = 0 \\ & \approx f(\hat{z}_i, \hat{x}_{i-1}) + \left.\frac{\partial f}{\partial z}\right|_{z=\hat{z}_i} (z_i - \hat{z}_i) + \left.\frac{\partial f}{\partial \hat{x}}\right|_{\hat{x}=\hat{x}_{i-1}} (\hat{x} - \hat{x}_{i-1}), \end{aligned} \tag{10}$$

where $\left.\frac{\partial f}{\partial z}\right|_{z=\hat{z}_i}$ and $\left.\frac{\partial f}{\partial \hat{x}}\right|_{\hat{x}=\hat{x}_{i-1}}$ represent the estimated value of $\frac{\partial f}{\partial z}$ and $\frac{\partial f}{\partial \hat{x}}$ at $\hat{z}_i$ and $\hat{x}_{i-1}$, respectively.

In a linear system, (10) can be rearranged as the following matrix equation [8]:

$$y_i = M_i \hat{x} + u_i, \tag{11}$$

where $y_i = -f(\hat{z}_i, \hat{x}_{i-1}) + \left.\frac{\partial f}{\partial \hat{x}}\right|_{\hat{x}=\hat{x}_{i-1}} \hat{x}_{i-1}$, $M_i = \left.\frac{\partial f}{\partial \hat{x}}\right|_{\hat{x}=\hat{x}_{i-1}}$, and $u_i = \left.\frac{\partial f}{\partial z}\right|_{z=\hat{z}_i} (z_i - \hat{z}_i)$.

In this equation, y_i is the new measured vector, M_i linearly combines the measured vector and the robot position, $\hat{x}$, and u_i is the error in linearization of the measured vector with the following average and variance values [6]:

$$E[u_i] = 0, \tag{12}$$

$$E[u_i u_i^T] = W_i = \frac{\partial \hat{f}}{\partial z} S_i \frac{\partial \hat{f}^T}{\partial z}. \tag{13}$$

Since M_i and y_i are a priori given values, if the average and variance of u_i are known, we can obtain the optimal estimated value of $\hat{x}$ with the new variance. The Kalman filter provides the estimated value, $\hat{x}$, which minimizes the expected squared error norm, $E[(\hat{x}-x)^T(\hat{x}-x)]$, as the linear combination of the measured vectors, $\{y_i\}$, as follows:

$$\hat{x}_i = \hat{x}_{i-1} + K_i(y_i - M_i \hat{x}_{i-1}), \tag{14}$$

$$K_i = P_{i-1} M_i^T (M_i P_{i-1} M_i^T + W_i)^{-1}, \tag{15}$$

$$P_i = (I - K_i M_i) P_{i-1}, \tag{16}$$

where K_i represents the Kalman gain, P_i is the zero-mean-variance matrix of the estimated error by the i[th] measured vector, and $\hat{x}_i$ is the estimated robot position by the i[th] measured vector.

The initial robot position estimation and variance, $\hat{x}_0$ and P_0, can be obtained using the mobile robot driving model. Using n image frames from the image coordinates of the moving object, the final robot position is recursively estimated as $\hat{x}_n$, with a variance of P_n.

4.3. State estimation of moving objects based on a Kalman filter

Input data such as image information include uncertainties and noises generated during the data capturing and processing steps. And the state transition of a moving object also includes irregular components. Therefore as a robust state estimator against these irregularities, a Kalman filter was adopted to form a state observer [9,10]. The Kalman filter minimizes the estimation error by modifying the state transition model based on the error between the estimated vectors and the measured vectors, with an appropriate filer gain. The state vector which consists of position on the x-y plane, linear/angular velocities, and linear/angular accelerations can be estimated using the measured vectors representing the position of a moving object on the image plane.

The covariance matrix of estimated error must be calculated to determine the filter gain. The projected estimate of the covariance matrix of estimated error is represented as

$$P_k' = \Phi_{k,k-1} P_{k-1} \Phi_{k,k-1}^T + Q_{k-1}, \tag{17}$$

where P_k' is a zero-mean covariance matrix representing the prediction error, Φ_k represents system noise, P_{k-1} is an error covariance matrix for the previous step, and Q_{k-1} represents other measurement and computational errors .

The optimal filter gain K_k that minimizes the errors associated with the updated estimate is

$$K_k = P_k' H_k^T [H_k P_k' H_k^T + R_k]^{-1}, \tag{18}$$

where H_k is the observation matrix and R_k is the zero-mean covariance matrix of the measurement noise.

The estimate of the state vector $\hat{x}_k$ from the measurement Z_k is expressed as

$$\hat{x}_k = \Phi_{k,k-1}\hat{x}_{k-1} + K_k[Z_k - H_k\Phi_{k,k-1}\hat{x}_{k-1}]. \quad (19)$$

Therefore, $\hat{x}_k$ is updated based on the new values provided by Z_k. The error covariance matrix that will be used for the prediction, P_k, can be updated as follows;

$$P_k = P_k' - K_k H_k P_k'. \quad (20)$$

After the current time is updated to $k+1$, a new estimation can be provided using (17) to (20). Fig. 8(a) represents a real and an estimated trajectory of a moving object, while Fig. 8(b) represents the estimation error when the trajectory was estimated by the Kalman filter. To incorporate the measurement noise which is empirically assumed to be zero-mean, Gaussian random noise with the variance of 2, the

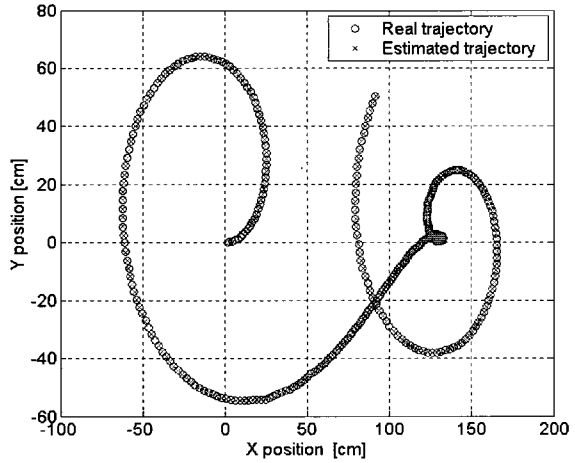

(a) Trajectory of moving object.

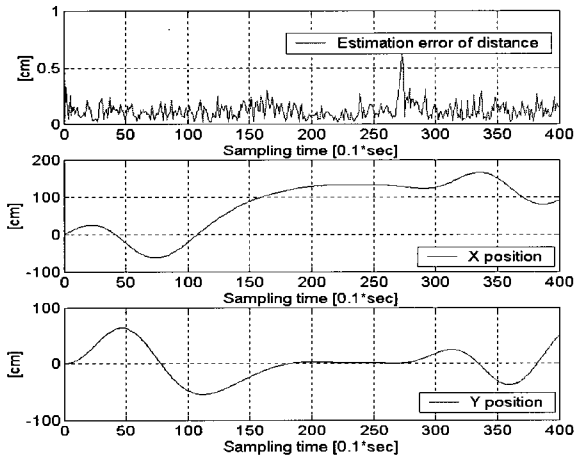

(b) Estimation error along the trajectory.

Fig. 8. State estimations using a Kalman filter.

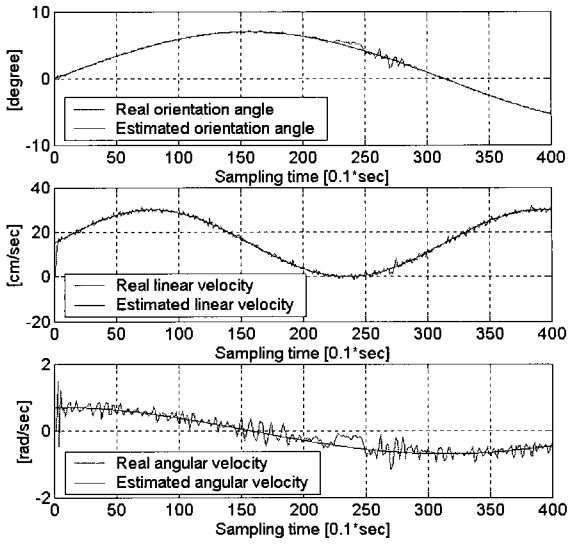

Fig. 9. State estimations, θ_k, v_k, and ω_k, using a Kalman filter.

linear and angular velocities of the object were set as follows:

$$\begin{aligned} v_k &= 16*(\sin(0.03*k)+1) + \xi_v \quad [\text{cm/sec}], \\ \omega_k &= 0.65*\cos(0.02*k) + \xi_\omega \quad [\text{rad/sec}], \end{aligned} \quad (21)$$

where the linear and angular velocities (ξ_v, ξ_w) were assumed to include the Gaussian random noise with the variance of 3 and 0.1, respectively.

Fig. 9 shows that the Kalman filter estimation of the states under a noisy environment.

5. SIMULATION AND EXPERIMENTS

5.1. Simulations

Simulations were performed for two different patterns of walking human motion: the parabolic motion and the sinusoidal motion. To achieve realistic conditions, the camera parameters listed in Table 1 were utilized:

The variances of the measured vectors were independent of each other, and the empirical variances were obtained as follows:

$$S_i = \begin{bmatrix} 0.005^2 & 0 \\ 0 & 0.005^2 \end{bmatrix}. \quad (22)$$

Table 1. Parameters of the camera system.

Parameter	Value
Camera height(h)	220cm
Focal length (λ)	1.25cm
CCD size (H)×(V)	0.66 cm × 0.48 cm

The estimated initial position and the error variance were obtained from a mobile robot driving model with a control cycle of 100 ms, in which the input errors of the wheel angle readings are limited to within 2% for Kalman filtering.

Case 1: Parabolic Walking Motion

As a simple example, an object was assumed to be moving along a parabolic curve specified by the range, $X_w = 400\text{cm} \sim 600\text{cm}$, $Y_w = -0.1(X_w - 500)^2 + 1200\text{cm}$, $Z_w = 100cm$, walking speed: 30 cm/s.

Fig. 10(a) and (b) represent the moving path of the walking human in 3-D space and on the image frame respectively, and Fig. 11 depicts the quantitative improvement of the position estimation uncertainty. Finally, Fig. 12 represents the position estimation error for each component of the robot position, (x, y, θ), when the parabolic walking motion is utilized for the localization. It should be noted that since the information of walking human is used for the position correction on the x-y plane, the uncertainty ellipsoid shrunk along all directions, as shown in Fig. 11. Moreover, as shown in Fig. 12, this causes both the x and y position errors of the robot to converge to zero. The position estimations and zero-mean variances before and after 100 iterations are shown as follows:

Initial: $\hat{x}_0 = [490\text{cm} \quad 480.5\text{cm} \quad 95°]^T$ and

$$P_0 = \begin{bmatrix} 243.1162 & -89.8719 & -0.6576 \\ -89.8719 & 62.9118 & 0.2529 \\ -0.6576 & 0.2529 & 0.0105 \end{bmatrix},$$

Final: $\hat{x}_{100} = [500.4\text{cm} \quad 499.6\text{cm} \quad 90.2°]^T$ and

$$P_{100} = \begin{bmatrix} 3.6294 & -2.1574 & 0.0080 \\ -2.1574 & 15.4273 & -0.0044 \\ 0.0080 & -0.0044 & 0 \end{bmatrix}.$$

It should be noted that the estimated position, $\hat{x}_{100}$=[500.4cm 499.6cm 90.2°]^T, converges precisely to the real position, $x = [500\text{cm} \quad 500\text{cm} \quad 90°]^T$.

Case 2: Sinusoidal Walking Motion

As a general case, the trajectory of a walking human was assumed to be a sinusoidal trajectory

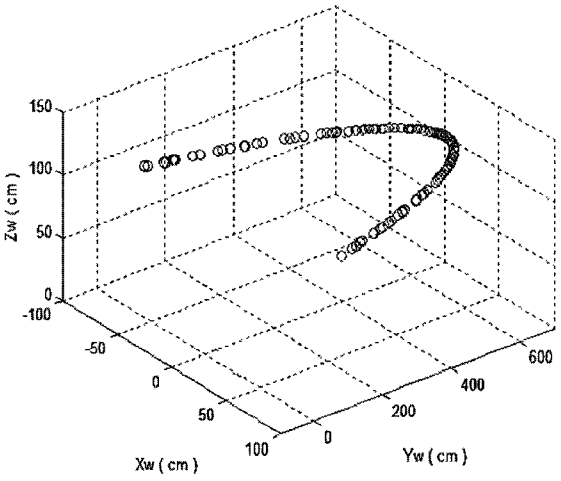

(a) Trajectory of moving object.

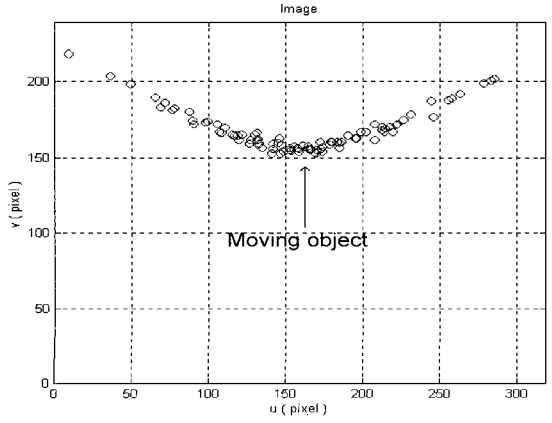

(b) Image coordinates of moving object.

Fig. 10. Moving object trace on the image frame.

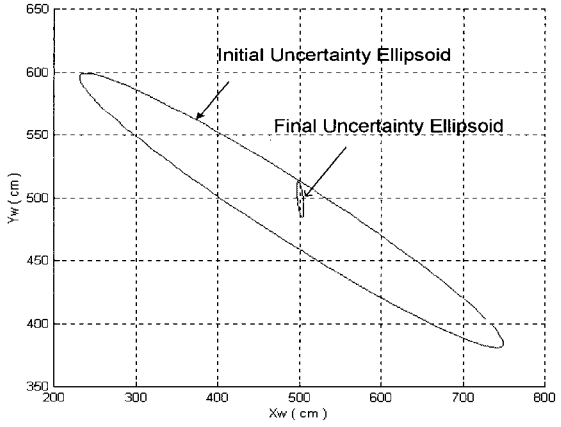

Fig. 11. Improvement of position estimation uncertainty.

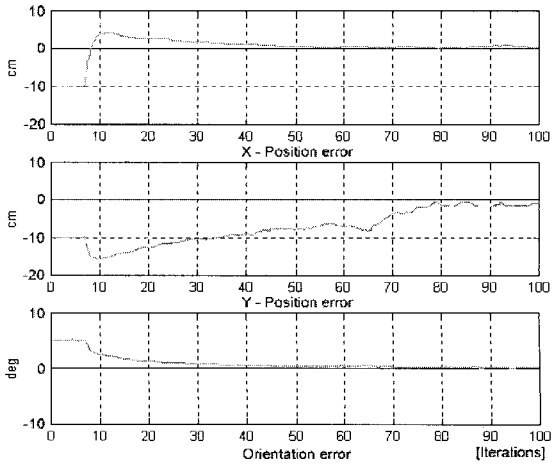

Fig. 12. Position estimation errors.

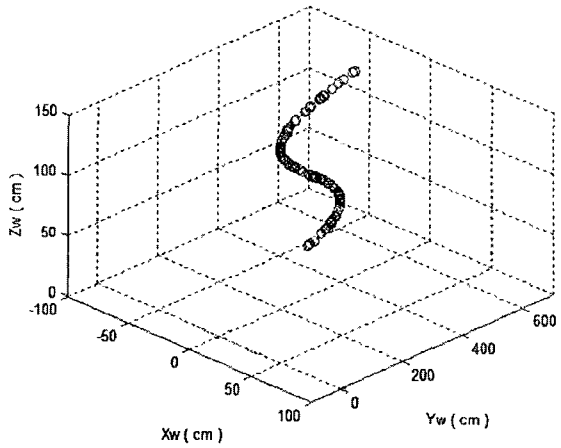

(a) Trajectory of moving object.

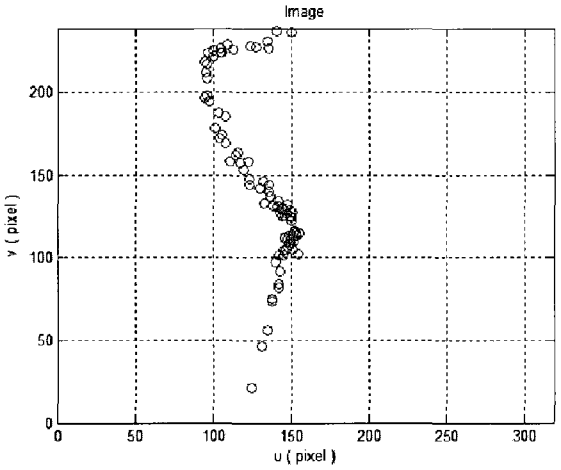

(b) Image coordinates of moving object.

Fig. 13. Moving object trace on the image frame.

represented as follows:

$X_w = 400\text{cm} \sim 600\text{cm}$, $Y_w = -0.01(X_w - 500)^3 + 300\text{cm}$, $Z_w = 100cm$, walking speed: 30 cm/s.

Fig. 13(a) and (b) represent the sinusoidal moving path of the walking human and the image coordinates of a moving object, respectively. Fig. 14 shows that the uncertainty ellipsoid for a moving object closer to the walking human tends to be smaller, as expected for visual information with updated estimation. Finally, Fig. 15 represents the position error and the orientation error for each component of the robot position. These simulation results indicate that the multi-visual estimations correspond well to the actual objects in the ISpace.

Initial: $\hat{x}_0 = [490\text{cm} \quad 480\text{cm} \quad 95°]^T$ and

$$P_0 = \begin{bmatrix} 242.9162 & -89.7719 & -0.5576 \\ -89.7719 & 62.3118 & 0.1829 \\ -0.5576 & 0.1829 & 0.0015 \end{bmatrix},$$

Final: $\hat{x}_{100} = [503.4\text{cm} \quad 504.0\text{cm} \quad 90.2°]^T$ and

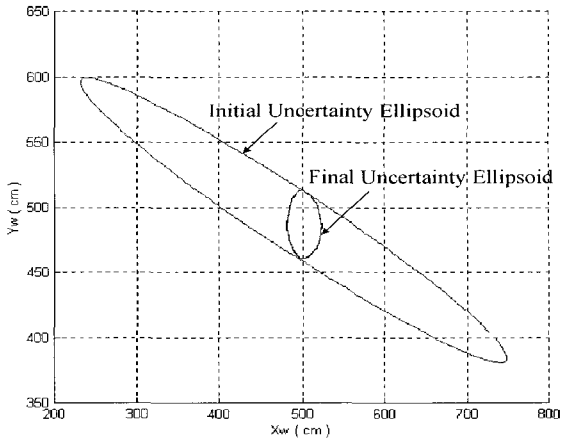

Fig. 14. Improvement of position estimation uncertainty.

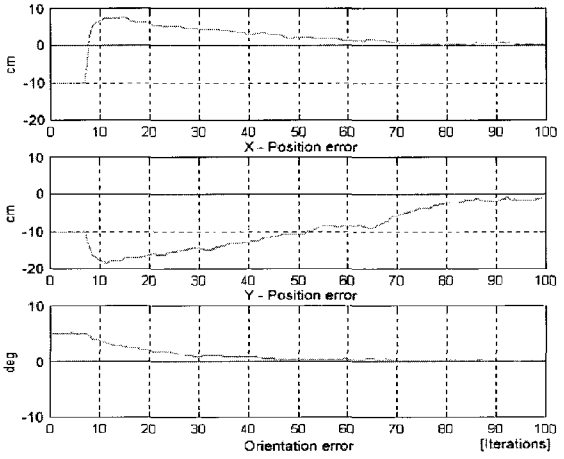

Fig. 15. Position estimatioan errors.

$$P_{100} = \begin{bmatrix} 5.7384 & -2.2684 & 0.0180 \\ -2.2684 & 15.8873 & -0.0174 \\ 0.0180 & -0.0174 & 0 \end{bmatrix}.$$

It should be noted that the estimated position, $\hat{x}_{100}$=[503.4cm 504.0cm 90.2°]^T, converges precisely to the real position, $x = [500\text{cm} \quad 500\text{cm} \quad 90°]^T$.

5.2. Experiments

As shown in Fig. 16, real experiments were performed in the ISpace. In this experiment, the robot was driven to follow a walking human in the ISpace. The initial position of the mobile robot was set to (0 cm, 0 cm, 90°) and the goal position to be achieved was (30 cm, 200 cm, 90°); the CCD camera of a DIND tracked the walking human on the floor to correct its own position. The trajectory of the walking human was captured by a color CCD camera, VC-C4R, manufactured by Canon Inc., and the traces were obtained as location (30 cm, 400 cm, 90°) to (80 cm, 250 cm, 0°) at a speed of 100 cm/s. The

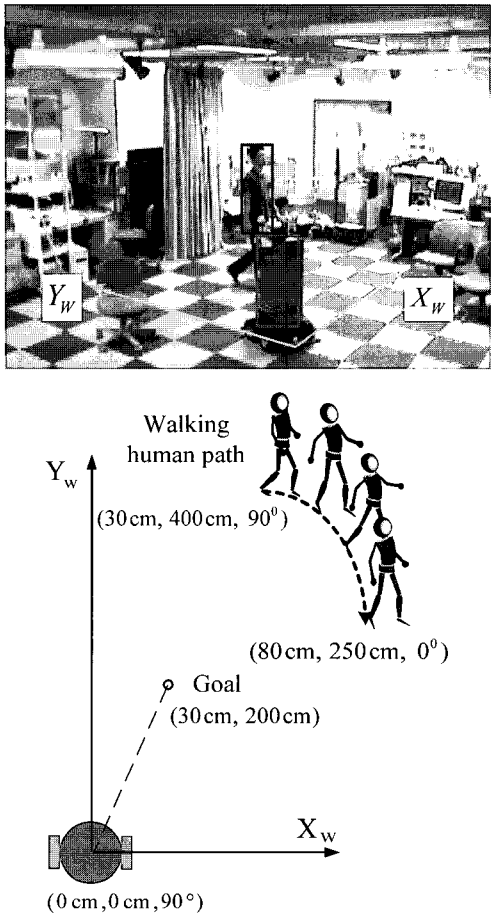

Fig. 16. Experimental environment.

parameters used for the experiments were the same as those used for the simulations. When the robot arrived at the goal position, it had captured 20 frames of images of the walking human at every 100 ms, and it utilized this information to estimate and correct its own position. The real position of the mobile robot was $[33\text{ cm}\quad 208\text{ cm}\quad 90°]^T$. The estimated position of the mobile robot and the variance of the estimated error are as follows:

$$\hat{x}_0 = [28\text{cm}\quad 195\text{cm}\quad 87.9°]^T \text{ and}$$

$$P_0 = \begin{bmatrix} 49.951 & -1.021 & -0.154 \\ -1.021 & 0.183 & 0.003 \\ -0.154 & 0.003 & 0.001 \end{bmatrix}.$$

After the 100 frames of observation, the estimated position of the mobile robot was approximately equal to the real position and the variance of the estimated error greatly reduced, as shown below:

$$\hat{x}_{100} = [29.4\text{cm}\quad 196.4\text{cm}\quad 89.7°]^T \text{ and}$$

$$P_{100} = \begin{bmatrix} 8.0406 & -0.1784 & 0.0252 \\ -0.1784 & 0.1660 & -0.0006 \\ 0.0252 & -0.0006 & 0.0001 \end{bmatrix}.$$

The robot position estimation uncertainty was represented as an uncertainty ellipsoid. It is rem`arkable that the size of the ellipsoid shrunk only along the normal direction of the walking human, as shown in Fig. 17(a). Fig. 17(b) shows the position errors of the mobile robot. As expected, it is evident that the position error reduces significantly as the robot moves, and it depended on the observed motion. The overall robot posture uncertainty for each cycle decreases over iterations, indicating that the estimation uncertainty reduces by observing the scene repeatedly with DINDs. Hence, a more accurate robot posture is obtained. Due to the above mentioned reason, the robot orientation decreases slightly when the walking motion does not include an acute angle turn.

These experiment results are obtained from experiments performed in the interior of the 7 m x 7 m space. Evidently, in the experiment, the experimental error range appears low since the mobile robot and walking human were assumed to be point objects, and

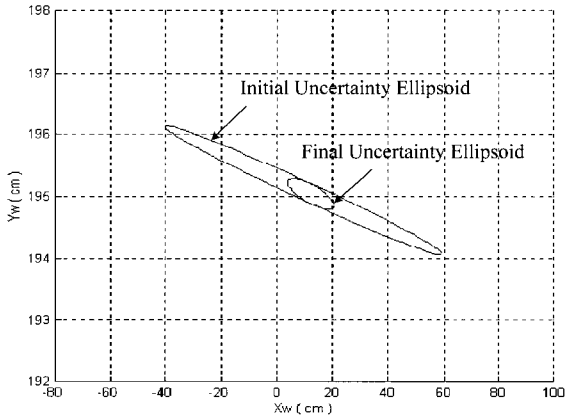

(a) Robot position estimation uncertainty.

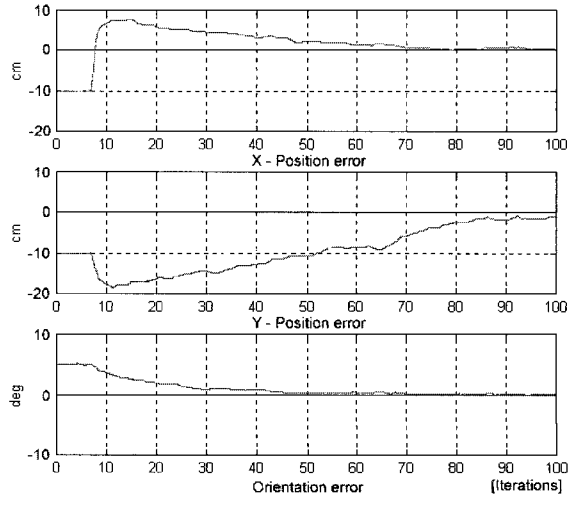

(b) Position errors.

Fig. 17. Improvement of position estimation uncertainty.

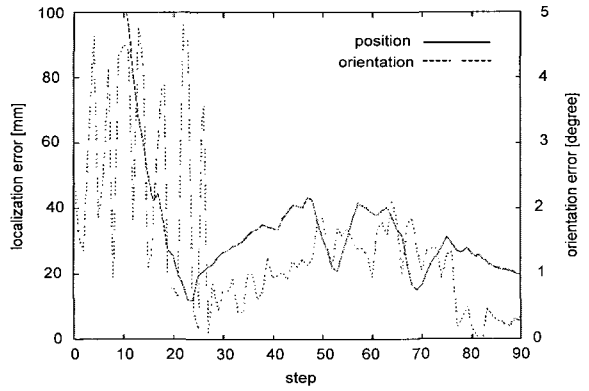

(a) Position and orientation estimation of a walking human.

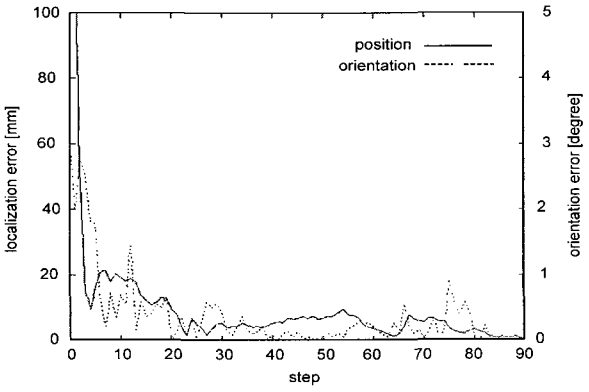

(b) Position and orientation estimation of a mobile robot.

Fig. 18. Experimental results obtained by DIND system.

the size of point was set to 30 cm x 100 cm. Fig. 18 presents additional experimental results when the walking speed is the same as in case 1. For the comparison purposes, the Kalman filter was designed based on case 1, and its outputs are plotted in the figure. The walking human moved along a parabolic trajectory in the x-y axis, and the motion models had the same zero-mean variance. Fig. 18(a) gives the experimental result when the average walking speed is 100 cm/s and the turns of the human are included. When the walking human accelerates, the DIND4, DIND5, and DIND6 are used to track the accurate position and direction of the human.

The response of the position is reasonably smooth, whereas the orientation θ continues to be very noisy during sampling step 30. This is due to distortions of the images caused by the human's motion and walking speed. During the sampling step of 90 ms, the error of position is at most 100 mm, and the error of orientation is up to 5 degrees. Fig. 18(b) shows the data plot of the robot localization error according to the motion information of walking human. Compared with Fig. 18(a), the response of the position is reasonably smooth. Moreover, when the average moving speed of mobile robot is 100 cm/s, the localization accuracy is reasonably high and the robot is able to quickly determine its absolute position in the environment.

In future research efforts, it is necessary to survey the influence of the mobile robot that maintains a flexible distance between the robot and the human. In the ISpace, since a human-walking trajectory is newly generated at every step, it can be considered to be a function of time. Therefore, the application of tracking control is effective. On the other hand, although the target trajectory of a mobile robot is continuous and smooth when the usual tracking control is used, the actual human-walking trajectory that is to be tracked by the robot is generally unstable. In such cases, stable human-following behavior may not be achieved by the usual tracking control is used.

6. CONCLUSION

In this paper, using the images of a walking human, an absolute position estimation method for a human-following robot in the ISpace was presented. First, the position estimation uncertainty of the mobile robot was quantitatively represented by the uncertainty ellipsoid. The real position of the human was transformed to geometric constraint equations in the image coordinates for a given robot position. Using the linear constraint equations and the Kalman filtering technique, the control algorithm was proposed for the mobile robot in order to estimate and correct its position recursively and enable it to follow a walking human whose position was incompletely estimated.

Specifically, the pre-determined path of a walking human is projected onto an image frame; then, the geometrical constraint equations between the coordinates of human's image and the estimated position of the human-following robot are derived. Since the location is based on the estimated position of the mobile robot, there exists a positional discrepancy between the estimated image coordinates and the real position of the walking human. Using this discrepancy, the position of the mobile robot was corrected recursively. Since the image coordinates of the human are subjected to noise, the Kalman filtering technique was adopted for robust estimation. Next, cooperation between the multiple DINDs was described. The positions of the human and the mobile robot in ISpace were measured by DINDs. To control a mobile robot over a wide area, cooperation of the DINDs, effective communication, and role assignment are required. Finally, simulations and an experiment on the human-following control of a mobile robot were performed using the proposed control algorithm. It was observed that position estimation accuracy depends on the path of the walking human. The

effectiveness of this algorithm was verified through real experiments.

Future studies will involve improving the estimation accuracy for the human-following robot and applying this system to complex environments where several people, mobile robots, and obstacles coexist. Real-time image processing and camera calibration are required to improve the estimation accuracy of the distance between the human and the mobile robot. Since the proposed algorithm absorbs the kinematic differences between the humans and robots, any type of mobile robot, including legged robots, can be used as a human-following robot, provided the robot is able to move at the walking speed of the human. Moreover, it is necessary to examine the influence of the mobile robot that maintains a flexible distance between the robot and the human, and introduces knowledge of cognitive science and social science into the study.

REFERENCES

[1] L. Moreno and E. Dapena, "Path quality measure for sensor-based motion planning," *Robotics and Autonomous Systems*, vol. 44, pp. 131-150, 2003.

[2] B. Bouilly and T. Siméon, "A sensor-based motion planner for mobile robot navigation with uncertainty," *Proc. of the International Workshop on Reasoning with Uncertainty in Robotics* (RUR), Springer, pp. 235-247, 1996.

[3] M. Betke and L. Gurvits, "Mobile robot localization using landmarks," *IEEE Trans. on Robotics and Automation,* vol. 13, no. 2, pp. 251-263, April 1997.

[4] D. J. Kriegman, E. Triendl, and T. O. Binford, "Stereo vision and navigation in buildings for mobile robots," *IEEE Trans. on Robotics and Automation*, vol. 5, no. 6, pp. 792-803, 1989.

[5] J. H. Lee, G. Appenzeller, and H. Hashimoto, "An agent for intelligent spaces: Functions and roles of mobile robots in sensored, networked, thinking spaces," *Proc. IEEE Conference Intelligent Transportation Systems*, Boston, pp. 983-988, 1997.

[6] Y. Nakamura, *Advanced Robotics: Redundancy and Optimization*, Addison-Wesley, 1991.

[7] R. M. Haralick and L. G. Shapiro, *Computer and Robot Vision*, Addison-Wesley, 1993.

[8] N. Ayache and O. D. Faugeras, "Maintaining representations of the environment of a mobile robot," *IEEE Trans. on Robotics and Automation*, vol. 5, no. 6, pp. 804-819, 1989.

[9] R. E. Kalman, "New approach to linear filtering and prediction problems," *Trans, ASME, J. Basic Eng*, Series 82D, pp. 35-45, March 1960.

[10] H. W. Sorenson, "Kalman filtering techniques," *Advances in Control Systems Theory and Applications*, vol. 3, pp. 219-292, 1966.

[11] M. Y. Han, B. K. Kim, K. H. Kim, and J. M. Lee, "Active calibration of the robot/camera pose using the circular objects," *Trans. on Control, Automation and Systems Engineering* (in Korean), vol. 5, no. 3, pp. 314-323, April 1999.

[12] T. Akiyama, J. H. Lee, and H. Hashimoto, "Evaluation of CCD camera arrangement for positioning system in intelligent space," *Proc. of Seventh International Symposium Artificial Life and Robotics*, pp. 310-315, 2002.

[13] D. Nair and J. K. Aggarwal, "Moving obstacle detection from a navigation robot," *IEEE Trans. Robotics and Automation*, vol. 14, no. 3, pp. 404-416, 1989.

[14] A. Lallet and S. Lacroix, "Toward real-time 2D localization in outdoor environments," *Proc. of the IEEE International Conference on Robotics & Automation*, pp. 2827-2832, May 1998.

[15] A. Adam, E. Rivlin, and I. Shimshoni, "Computing the sensory uncertainty field of a vision-based localization sensor," *Proc. of the IEEE International Conference on Robotics & Automation*, pp. 2993-2999, April 2000.

[16] R. Sim and G. Dudek, "Learning visual landmarks for pose estimation," *Proc. of the IEEE International Conference on Robotics & Automation*, pp. 1972-1978, May 1999.

[17] B. H. Kim, D. K. Roh, J. M. Lee, M. H. Lee, K. Son, M. C. Lee, J. W. Choi, and S. H. Han, "Localization of a mobile robot using images of a moving target," *Proc. of the IEEE International Conference on Robotics & Automation*, pp. 253-258, May 2001.

[18] V. Caglioti, "An entropic criterion for minimum uncertainty sensing in recognition and localization part II-A case study on directional distance measurements," *IEEE Trans. on Systems, Man, and Cybernetics*, vol. 31, no. 2, pp. 197-214, April 2001.

[19] C. F. Olson, "Probabilistic self-localization for mobile robots," *IEEE Trans. on Robotics and Automation*, vol. 16, no. 1, pp. 55-66, Feb. 2000.

[20] H. Zhou and S. Sakane, "Sensor planning for mobile robot localization based on probabilistic inference using bayesian network," *Proc. of the 4th IEEE International Symposium on Assembly and Task Planning*, pp. 7-12, May 2001.

[21] M. Selsis, C. Vieren, and F. Cabestaing, "Automatic tracking and 3D localization of moving objects by active contour models," *Proc. of the IEEE International Symposium on Intelligent Vehicles*, pp. 96-100, 1995.

[22] H. Choset and K. Nagatani, "Topological simultaneous localization and mapping (SLAM): Toward exact localization without explicit localization," *IEEE Trans. on Robotics and*

Automation, vol. 17, no. 2, pp. 125-137, April 2001.

[23] S. Segvic and S. Ribaric, "Determining the absolute orientation in a corridor using projective geometry and active vision," *IEEE Trans. on Industrial Electronics*, vol. 48, no. 3, pp. 696-710, June 2001.

[24] P. Hoppernot and E. Colle, "Localization and control of a rehabilitation mobile robot by close human-machine cooperation," *IEEE Trans. on Neural Systems and Rehabilitation Engineering*, vol. 9, no. 2, pp. 181-190, June 2001.

[25] J. H. Lee and H. Hashimoto, "Intelligent space - concept and contents," *Advanced Robotics*, vol. 16, no. 3, pp. 265-280, 2002.

[26] J. H. Lee and H. Hashimoto, "Mobile robot control by distributed sensors," *Proc. of IFAC Workshop Mobile Robot Technology*, pp. 85-90, 2001.

Tae-Seok Jin received the B.Sc. degree in Jinju National University, M.Sc. and Ph.D. degrees in Pusan National University, Korea, in 2000 and 2003, respectively, all in Electronics Engineering. From 2004 to 2005, he was a Postdoctoral Researcher at the Institute of Industrial Science, The University of Tokyo, Japan. He is currently a Full-time Lecturer at the Dept. of Mechatronics Engineering, DongSeo University. His research interests include intelligent space with multi-sensor fusion, mobile robot control. Dr. Jin is a Member of the JSME, IEEK, ICASE, and KFIS.

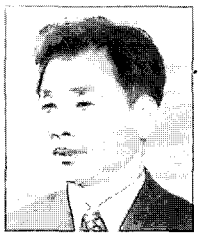

Jang-Myung Lee has been a Professor in the Department of Electronics Engineering, Pusan National University. He received the B.Sc. and the M.Sc. degrees in Electronics Engineering from Seoul National University in 1980 and 1982, respectively and the Ph.D. degree in Computer Electronics from the USC in 1990. His current research interests include intelligent robotic systems, integrated manufacturing systems, and cooperative control. Prof. Lee is an IEEE Senior member, and a member of ICASE and IEEK.

Hideki Hashimoto received the B.E., M.E., and Dr. Engineering degrees in Electrical Engineering from The University of Tokyo, Tokyo, Japan, in 1981, 1984, and 1987, respectively. He is currently an Associate Professor at the Institute of Industrial Science, The University of Tokyo. From 1989 to 1990, he was a Visiting Researcher at Massachusetts Institute of Technology, Cambridge. His research interests are control and robotics, in particular, advanced motion control and intelligent control. Prof. Hashimoto is a Member of the SICE, IEEE, and RSJ.